

# Beyond Miransky Scaling

Jens Braun,<sup>1</sup> Christian S. Fischer,<sup>2</sup> and Holger Gies<sup>1</sup>

<sup>1</sup>*Theoretisch-Physikalisches Institut, Friedrich-Schiller-Universität Jena, Max-Wien-Platz 1, D-07743 Jena, Germany*

<sup>2</sup>*Institut für Theoretische Physik, Justus-Liebig-Universität Giessen, Heinrich-Buff-Ring 16, 35392 Giessen, Germany*

We study the scaling behavior of physical observables in strongly-flavored asymptotically free gauge theories, such as many-flavor QCD. Such theories approach a quantum critical point when the number of fermion flavors is increased. It is well-known that physical observables at this quantum critical point exhibit an exponential scaling behavior (Miransky scaling), provided the gauge coupling is considered as a constant external parameter. This scaling behavior is modified when the scale dependence of the gauge coupling is taken into account. Provided that the gauge coupling approaches an IR fixed point, we derive the resulting *universal* power-law corrections to the exponential scaling behavior and show that they are uniquely determined by the IR critical exponent of the gauge coupling. To illustrate our findings, we compute the universal corrections in many-flavor QCD with the aid of nonperturbative functional renormalization group methods. In this case, we expect the power-law scaling to be quantitatively more relevant if the theories are probed, for instance, at integer  $N_f$  as done in lattice simulations.

## I. INTRODUCTION

Strongly-flavored asymptotically free theories, such as QCD and QED<sub>3</sub> are currently very actively researched. In particular, QCD with many quark flavors has drawn a lot of attention in recent years. On the one hand, the number of (massless) fermions can be considered as an external parameter. Such gauge theories are then expected to exhibit a quantum phase transition from a chirally broken to a conformal phase when the number of fermion flavors is increased. On the other hand, the understanding of strongly-flavored gauge theories underlies (walking) technicolor-like scenarios for the Higgs sector, see e. g. Refs. [1–9].

The phase structure of gauge theories with  $N_f$  fermions can indeed be rich, as simple considerations may already suggest. Due to the screening property of fermionic fluctuations, asymptotic freedom is lost for large  $N_f$ . For instance, SU( $N_c$ ) gauge theory with  $N_f$  fermions is no longer asymptotically free (a.f.) for  $N_f > N_f^{\text{a.f.}} := \frac{11}{2}N_c$ . Another special fermion number  $N_f^{\text{CBZ}}$  potentially exists denoting the minimum flavor number for the occurrence of an infrared fixed point  $g_*^2$  of the running gauge coupling. For instance, the two-loop  $\beta$  function of the gauge coupling  $g^2$  exhibits the so-called Caswell-Banks-Zaks (CBZ) fixed point [10], as the screening nature of fermion fluctuations dominates the two-loop coefficient for  $N_f > N_f^{\text{CBZ}}$ . For instance for SU(3), we have  $N_f^{\text{CBZ}} \simeq 8.05$  in the two-loop approximation. A perturbative treatment of the theory seems possible near  $N_f^{\text{a.f.}}$ ,  $N_f \lesssim N_f^{\text{a.f.}}$ , where  $g_*^2$  is small, indicating the existence of a conformally invariant limit in the deep infrared [11]. For decreasing  $N_f$ ,  $g_*^2$  becomes larger, suggesting the onset of chiral symmetry breaking. The decoupling of massive fermions then destabilizes the Caswell-Banks-Zaks fixed point  $g_*^2$  in the gauge sector of the theory. The infrared of the theory is then dominated by massless bosonic excitations, the Goldstone modes, and the spectrum of

the theory is characterized by a dynamically generated mass gap. A similar reasoning also applies to QED<sub>3</sub>, see e. g. [12, 13].

These considerations suggest the existence of a *quantum critical point* associated with a critical flavor number  $N_f^{\text{CBZ}} \leq N_{f,\text{cr}} < N_f^{\text{a.f.}}$  above which gauge theories approach a conformally invariant limit in the infrared. Thus,  $N_f$  serves as a control parameter for the quantum phase transition.

Studies of the phase structure of strongly-flavored gauge theories have been performed employing continuum methods as well as lattice simulations. In QED<sub>3</sub> many studies have performed estimates to determine  $N_{f,\text{cr}}$  using Dyson-Schwinger equations and resummation techniques [12–22]. Since the dynamically generated mass is substantially smaller than the scale set by the gauge coupling, lattice simulations of QED<sub>3</sub> with many flavors are remarkably challenging [23–26]. The phase structure of many-flavor QCD has also been studied employing continuum methods [10, 11, 27–43], as well as lattice simulations [44–58]. Recent results suggest in this case that a conformal phase indeed exists with a quantum phase transition occurring near  $9 \lesssim N_{f,\text{cr}} \lesssim 13$ .

Given the existence of such a quantum critical point in an asymptotically free gauge theory with  $N_f$  flavors, the question arises how the spectrum of the theory behaves when we approach this quantum critical point from below. This question is tightly bound to the question of the  $N_f$  dependence of the dynamically generated scale associated with chiral symmetry breaking. It is well-known from studies of Dyson-Schwinger equations in the rainbow-ladder approximation that physical observables, e. g. the fermion condensate, exhibit an exponential scaling close to  $N_{f,\text{cr}}$ , provided that the (momentum) scale dependence of the gauge coupling can be neglected [28, 59–61],

$$k_{\text{SB}} \propto \Lambda \theta(N_{f,\text{cr}} - N_f) \exp \left( - \frac{\pi}{2\epsilon \sqrt{\alpha_1 |N_{f,\text{cr}} - N_f|}} \right). \quad (1)$$

Here,  $k_{\text{SB}}$  denotes a scale characteristic for the onset of symmetry breaking, being directly proportional, say, to a symmetry-breaking condensate. The quantities  $\epsilon$  and  $\alpha_1$  are pure constants arising from the details of the theory and will be defined below. This behavior can be viewed as a generalization of essential Berezinskii-Kosterlitz-Thouless (BKT) scaling [62–64] to higher dimensional systems [65]. We rush to add that the spectrum of the different theories below and above  $N_{\text{f,cr}}$  are substantially different. In particular, a construction of an effective low-energy theory in terms of light scalar fields may no longer be possible above  $N_{\text{f,cr}}$ .

Taking into account the running of the gauge coupling and going beyond the standard rainbow-ladder approximation, the scaling behavior of physical observables close to  $N_{\text{f,cr}}$  has been analyzed in [37, 38, 66]. More precisely, the  $N_{\text{f}}$  dependence of a strict upper bound for the symmetry breaking scale has been studied, scaling according to a power law,

$$k_{\text{cr}} \propto \Lambda |N_{\text{f,cr}} - N_{\text{f}}|^{-\frac{1}{\Theta_0}}. \quad (2)$$

Here,  $k_{\text{cr}}$  denotes the scale where the dynamics leading to symmetry breaking becomes critical. This means that operators that trigger symmetry breaking become relevant in an RG sense. As the system still has to run towards lower energy scales into the broken phase, we have  $k_{\text{cr}} > k_{\text{SB}}$ , implying that Eq. (2) is an upper bound for Eq. (1). Near the critical flavor number the corresponding scaling exponent is uniquely determined by the critical exponent  $\Theta_0$  of the gauge coupling at its infrared fixed point. This upper bound for the (chiral) symmetry breaking scale can be translated into an upper bound for physical observables [66]. In fact, the chiral phase-transition temperature as a function of the “external” control parameter  $N_{\text{f}}$  has been computed with non-perturbative functional renormalization group methods. The scaling of the phase boundary has been found to be compatible with the analytically derived scaling behavior [37, 38].

Recently, the scaling behavior of physical observables has been investigated again with the aid of Dyson-Schwinger equations in the rainbow-ladder approximation also taking into account part of (momentum) scale dependence of the gauge coupling by a proper adjustment of the scale [67]. It was then found that the exponential scaling behavior close to  $N_{\text{f,cr}}$  of the symmetry breaking scale is supplemented by a power-law behavior similar to the one found in Ref. [37, 38, 66].

In the present work, we aim to reveal the relation between these supposedly different scaling laws and show rigorously what kind of scaling behavior we should expect close to the quantum critical point of asymptotically free gauge theories with many flavors. Our arguments are based on very general RG considerations and involve only a few assumptions about the underlying fixed-point structure of the theory under consideration. In fact, we shall show that the above-given scaling laws arise as two different limits of one and the same RG flow. In addition,

we point out the importance of the scale-fixing procedure applied in the first place in order to compare theories with different flavor numbers. As the scaling behavior of the low-energy observables is accessible to a variety of nonperturbative methods, we believe that a rigorous understanding of scaling behavior near the phase transition to the conformal phase will be very useful.

In Sect. II, we briefly repeat the arguments that lead to an exponential scaling behavior at the quantum phase transition. In addition, we derive the leading-order correction to the exponential scaling behavior. In Sect. III, we then discuss the issue of scale fixing underlying a meaningful comparison between theories with different flavor numbers. Moreover, we briefly review the arguments from Refs [37, 38, 66] which lead to a power-law-like scaling behavior for a strict upper bound for the (chiral) symmetry breaking scale. In Sect. IV we then discuss the interrelation of the scaling laws put forward in Refs. [38, 59, 66, 67] and derive the leading-order scaling behavior of a given infrared observable at the quantum critical point. To illustrate our analytic findings, we present numerical results from a non-perturbative functional renormalization group study of the scaling behavior in many-flavor QCD in Sect. V.

## II. MIRANSKY SCALING

In this section we study exponential scaling behavior in gauge theories near a *quantum critical point*, also known as Miransky scaling [27, 59].

We shall keep our discussion as general as possible. For our purposes, however, we consider a general class of theories where symmetry breaking and condensate formation is driven by fermionic self-interactions. Independently of whether these interactions may be fluctuation-induced (as in QCD) or fundamental, this class of theories can be parameterized by the following action:

$$S_M = \int d^d x \left\{ \bar{\psi} (i\partial + \bar{g}A) \psi + \bar{\lambda}_{\alpha\beta\gamma\delta} \bar{\psi}_\alpha \psi_\beta \bar{\psi}_\gamma \psi_\delta \right\}, \quad (3)$$

where  $\alpha, \beta \dots$  denote a specific set of collective indices including, e. g., flavor and/or color indices. In general, we expect to have more than just one four-fermion interaction channel, see e. g. Sect. V for QCD with many flavors. Note that symmetry breaking is ultimately triggered by the interactions approaching criticality, i.e., becoming RG relevant.

Here and in the following we do not allow for terms in the action which explicitly break the underlying symmetry, such as current quark mass terms in QCD<sup>1</sup>.

---

<sup>1</sup> The scaling behavior of observables with the (current) quark mass in the (quasi-)conformal phase of strongly-flavored gauge theories is of particular interest for lattice simulations and currently under investigation, see Refs. [68–70].

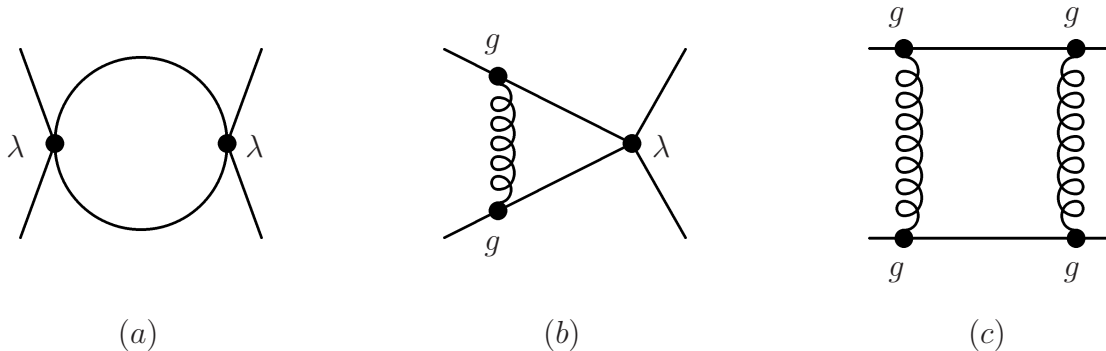


Figure 1: Representation of the terms on the right-hand side of the RG flow equation (4) by means of Feynman diagrams. Our functional RG studies, see Sect. V, include resummations of all diagram types including ladder-diagrams generated by type (b) and (c) as well as the corresponding crossed-ladder topologies.

From the action (3) we can derive the  $\beta$  function of the dimensionless four-fermion coupling  $\lambda$ . It assumes the following simple form:

$$\beta_\lambda \equiv \partial_t \lambda = (d-2)\lambda - a\lambda^2 - b\lambda g^2 - cg^4. \quad (4)$$

Here,  $t = \ln(k/\Lambda)$  denotes the RG 'time' with  $k$  being the RG scale and  $\Lambda$  being a UV cutoff scale. The couplings  $\lambda \sim \bar{\lambda}/k^{(d-2)}$  and  $g \sim \bar{g}/k^{4-d}$  denote dimensionless and suitably renormalized couplings. The first term in Eq. (4) arises from simple dimensional rescaling. The quantities  $a$ ,  $b$  and  $c$  do not depend on the RG scale but may depend on control parameters, such as the number of quark flavors  $N_f$  or the number of colors  $N_c$ .<sup>2</sup> The various terms on the right-hand side of Eq. (4) can be understood in terms of perturbative Feynman diagrams [71], see Fig. 1. Equation (4) can also be derived from nonperturbative flow equations in the limit of point-like (momentum-independent) interactions, see Sect. V. Note that we have dropped terms proportional to the anomalous dimension of the fermionic fields in Eq. (4). We assume these contributions to be small in the following. This is indeed the case in the chirally symmetric regime of QCD, at least in the Landau gauge [72].

In Eq. (3) we have not further specified the gauge sector. In fact, let us ignore the running of the gauge coupling in this section, and consider the gauge coupling as a *scale-independent* "external" parameter. The RG flow of the gauge coupling is then trivially governed by

$$\partial_t g^2 \equiv 0. \quad (5)$$

For example, this may be an acceptable approximation in the vicinity of an IR fixed point  $g_*^2$ . Note that the value of  $g_*^2$  may depend on other control parameters such as

<sup>2</sup> Note that the coefficients  $a$ ,  $b$  and  $c$  can depend implicitly on the RG scale as soon as we introduce a dimensionful external parameter, e. g., temperature  $T$ . However, the coefficients remain dimensionless since they depend only on the ratio  $T/k$ , see e. g. [37, 38].

$N_f$  or  $N_c$ , cf. our discussion of QCD with many flavors in Sect. V.

In Fig. 2 we show a sketch for the  $\beta_\lambda$  function, implicitly assuming that  $a > 0$ ,  $b > 0$  and  $c > 0$  in Eq. (4). For a vanishing gauge coupling  $g^2$  we find two fixed points, an IR attractive Gaussian fixed point at  $\lambda = 0$  and an IR repulsive fixed point at  $\lambda > 0$ . For increasing  $g^2$  these fixed points approach each other and eventually merge for a *critical* value  $g_{cr}^2$ ,

$$g_{cr}^2 = \frac{d-2}{b+2\sqrt{ac}}. \quad (6)$$

For  $g^2 > g_{cr}^2$  the four-fermion coupling then becomes a relevant operator and increases rapidly towards the IR indicating the onset of (chiral) symmetry breaking. Thus, the four-fermion coupling  $\lambda$  necessarily<sup>3</sup> diverges for  $g^2 > g_{cr}^2$  at a finite RG scale  $k_{SB} = k_{SB}(g^2)$ . This divergence is, of course, an artifact of the over-simplistic approximation (3), but can be related to a symmetry-breaking transition in the effective Landau-Ginzburg-type potential for fermion-bound states. Even though  $k_{SB}$  is not a direct observable, it sets the scale for observables such as condensates, decay constants, critical temperatures, etc. This picture of the emergence of chiral symmetry has been put forward in [36–38, 66] and successfully employed for an analysis of the phase structure of QCD with various numbers of flavors and colors at zero and finite temperature [36–38, 66]. Moreover, this picture has also been employed to study conformal scaling in quantum field theories, see e. g. Ref. [65].

<sup>3</sup> Here, we assume that the initial conditions at the UV scale  $k = \Lambda$  for the four-fermion coupling  $\lambda$  are chosen such that  $\lambda_\Lambda$  is smaller than the value of the IR repulsive fixed point, see Fig. 2. In beyond-standard model applications  $\lambda_\Lambda$  is sometimes considered to be a finite parameter, see e. g. [73]. We therefore add that the exponential scaling behavior discussed below can only be observed when  $\lambda_\Lambda$  is chosen to be smaller than the value of the repulsive fixed point for a given  $g^2$ . Otherwise, we expect a power-law-like scaling behavior [74].

Let us now briefly discuss the scaling behavior of the symmetry-breaking scale  $k_{\text{SB}}$  when  $g^2$  is varied by hand as a constant "external" parameter. To this end, we have to solve the RG flow equation (4). We find:

$$\ln k - \ln \Lambda = - \frac{2 \arctan \left( \frac{bg^2 - (d-2) + 2a\lambda'}{\delta(g^2)} \right)}{\delta(g^2)} \bigg|_{\lambda_{\text{UV}}}^{\lambda} \quad (7)$$

with

$$\delta(g^2) = \sqrt{4acg^4 - ((d-2) - bg^2)^2}. \quad (8)$$

Here and in the following we assume  $b > 0$  without loss of generality. From Eq. (7), we obtain  $k_{\text{SB}}$  by solving for the zero of  $1/\lambda(k)$ , i. e.  $1/\lambda(k_{\text{SB}}) = 0$ :

$$\ln k_{\text{SB}} - \ln \Lambda = - \frac{\pi}{\delta(g^2)} + \text{const.} \quad (9)$$

Here, we have chosen the initial conditions such that  $\lambda_{\text{UV}} = \lambda_{\text{max}}$  where  $\lambda_{\text{max}}$  denotes the position of the maximum of the  $\beta_\lambda$  function, i.e., the peak of the parabola in Fig. 2. An expansion of (9) around  $g_{\text{cr}}^2$  yields<sup>4</sup>

$$k_{\text{SB}} \propto \Lambda \theta(g^2 - g_{\text{cr}}^2) \exp \left( - \frac{\pi}{2\epsilon \sqrt{(g^2 - g_{\text{cr}}^2)}} \right), \quad (10)$$

where  $\epsilon$  is a numerical factor,

$$\epsilon = \sqrt{\frac{(d-2)(2ac + b\sqrt{ac})}{b + 2\sqrt{ac}}}, \quad (11)$$

which in general depends on the details of the theory under consideration, e. g. the number of colors and flavors in QCD. In any case, we find an exponential Miransky-scaling behavior of  $k_{\text{SB}}$  for  $g^2$  close to  $g_{\text{cr}}^2$ . Since the dynamically generated scale  $k_{\text{SB}}$  sets the scale for the low-energy sector, we expect that all IR observables  $\mathcal{O}$  scale according to:

$$\mathcal{O} = f_{\mathcal{O}} k_{\text{SB}}^{d_{\mathcal{O}}}, \quad (12)$$

where  $d_{\mathcal{O}}$  is the canonical mass dimension of the observable  $\mathcal{O}$  and  $f_{\mathcal{O}}$  is a function which does not depend on  $g_{\text{cr}}^2$  but may depend on  $g^2$  and other external parameters, e. g.,  $N_f$  and/or  $N_c$ . The function  $f_{\mathcal{O}}$  can be computed systematically within certain approximations schemes such as large- $N_c$  expansions or chiral perturbation theory, see e. g. [66, 67]. In the context of QCD the scaling law in Eq. (10) has been first derived by Miransky [27, 59] but has also been found in the context of specific 2-dimensional condensed-matter systems [64].

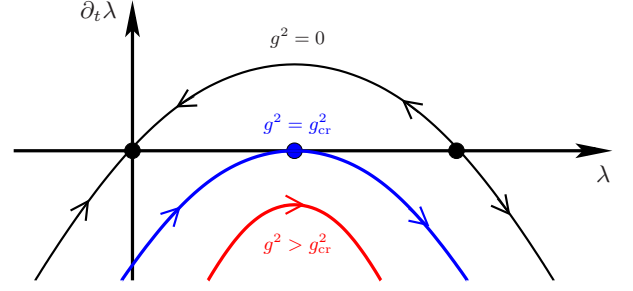


Figure 2: Sketch of a typical  $\beta$  function for the fermionic self-interactions  $\lambda$ , see [36] and also [38] for a generalization to finite temperature): at zero gauge coupling,  $g^2 = 0$  (upper black curve), the Gaussian fixed point  $\lambda = 0$  is IR attractive. For  $g^2 = g_{\text{cr}}^2$  (middle/blue curve), the fixed-points merge due to a shift of the parabola induced by the gauge-field fluctuations  $\sim g^4$ . For gauge couplings larger than the critical coupling  $g^2 > g_{\text{cr}}^2$  (lower/red curve), no fixed points remain and the self-interactions rapidly grow large, signaling chiral symmetry breaking. The arrows indicate the direction of the flow towards the infrared.

The derivation of the scaling law (10) via an analysis of the RG flow of four-fermion operators has been recently pointed out by Kaplan, Lee, Son and Stephanov [65].

Let us now briefly discuss the consequences of the scaling law (10) when we apply our considerations to strongly-flavored gauge theories, such as QCD with many quark flavors or QED<sub>3</sub>. In these cases we may choose the IR fixed-point of the gauge coupling as an external parameter, i. e.  $g^2 = g_*^2(N_f)$  in Eq. (10). Depending on the  $N_f$  dependence of the coefficients  $a$ ,  $b$  and  $c$  in the  $\beta_\lambda$  function, the critical value for the gauge coupling may depend on the number of flavors as well,  $g_{\text{cr}}^2 = g_{\text{cr}}^2(N_f)$ . The critical number of quark flavors  $N_{f,\text{cr}}$  can then be obtained from the criticality condition

$$g_{\text{cr}}^2(N_{f,\text{cr}}) = g_*^2(N_{f,\text{cr}}). \quad (13)$$

This corresponds to the coupling value for which the two fixed points of the four-fermion coupling  $\lambda$  merge and then annihilate each other for  $g^2 > g_{\text{cr}}^2$ . Expanding  $g_*^2(N_f) - g_{\text{cr}}^2(N_{f,\text{cr}})$  around  $N_{f,\text{cr}}$ ,

$$g_*^2(N_f) - g_{\text{cr}}^2(N_{f,\text{cr}}) = \alpha_1 (N_f - N_{f,\text{cr}}) + \alpha_2 (N_f - N_{f,\text{cr}})^2 + \dots, \quad (14)$$

and plugging (14) into (10), we find the exponential  $N_f$  scaling of  $k_{\text{SB}}$ :

$$k_{\text{SB}} \propto \Lambda \theta(N_{f,\text{cr}} - N_f) \exp \left( - \frac{\pi(1 - \frac{\alpha_2}{\alpha_1} |N_{f,\text{cr}} - N_f| + \dots)}{2\epsilon \sqrt{\alpha_1 |N_{f,\text{cr}} - N_f|}} \right). \quad (15)$$

Whether the size of the regime for exponential scaling is small depends on the ratio  $\alpha_2/\alpha_1$  which in turn depends on the theory under consideration. Thus, the size of the scaling regime may presumably be different in, e. g., QCD and QED<sub>3</sub>. In Sect. V we compare the analytic findings of this section with results from a numerical analysis of QCD with many flavors.

<sup>4</sup> Note that  $g_{\text{cr}}^2$  is defined to be the value of  $g^2$  for which the  $\beta_\lambda$  function has exactly one zero. In general there exist two solutions for  $g_{\text{cr}}^2$ , however, one of which can be excluded from a physical point of view.



### III. POWER-LAW SCALING

In this section we discuss how the running of the gauge coupling affects the RG flow of the four-fermion coupling(s). In particular, we argue that (chiral) symmetry breaking in strongly-flavored gauge theories is a multi-scale problem, in contrast to the scenario discussed in the previous section. In other words, the (chiral) symmetry breaking scale  $k_{\text{SB}}$  discussed above and its scaling with the control parameters, e. g. the number of flavors  $N_f$ , depends on the scale fixing and its potential flavor dependence.

In the following, we include the running of the gauge coupling which goes beyond standard rainbow-ladder approaches employed in the context of strongly-flavored gauge theories, see e. g. Ref. [32].

Since we are eventually interested in the scaling behavior of IR observables, e. g. the fermion condensate, it is important to realize that a variation of the flavor number does not quite correspond to a change of a parameter of the theory. It rather corresponds to changing the theory itself. We would like to stress that there is indeed no unique way to unambiguously compare theories of different flavor number with each other, as different theories may be fixed at different scales.

As we have argued in more detail in Ref. [66], fixing the scale of theories with, say, different flavor numbers  $N_f$  by keeping the running coupling at some scale  $\Lambda$  (e. g.  $\tau$  mass) fixed to a certain value, seems to be a well accessible prescription for many non-perturbative methods. In general, it is important to take care that this scale-fixing procedure is not (or as little as possible) spoiled by scheme dependencies. The latter constraint essentially rules out  $\Lambda_{\text{QCD}}$  as a proper scale in QCD to be kept fixed in theories with different flavor numbers. Of course, it is also possible, e. g. in lattice QCD simulations, to keep the value of an IR observable fixed for theories with different  $N_f$ , e. g. the pion decay constant or the critical temperature. We shall briefly comment on such a procedure below. For what follows, however, we choose a mid-momentum scale for the scale fixing, lying in between the high-scale perturbative running and the more interesting non-perturbative dynamics. Thus, we fix the theories at any  $N_f$  by keeping the running coupling at some intermediate scale  $\Lambda$  fixed to a certain value, say  $\alpha_\Lambda$ .

To be more specific, we shall focus our discussion on strongly-flavored asymptotically free gauge theories, such as QCD with many flavors and  $\text{QED}_3$ .<sup>5</sup> In such theories, the dependence of the running coupling on the scale and on further control parameters such as  $N_f$  is expected to modify Miransky scaling. In particular, an understanding of the universal scaling behavior of observables in the

ordered phase close to the phase transition at  $N_{f,\text{cr}}$  is of interest. However, the arguments also apply to other theories in which dynamical chiral symmetry breaking is triggered by a running coupling which approaches a non-trivial IR fixed point.

For a monotonically increasing coupling flow, the value of the non-trivial IR fixed point  $g_*^2$  of the gauge coupling corresponds to the maximum possible coupling strength of the system in the conformal window, i. e. for  $N_{f,\text{cr}} < N_f < N_f^{\text{a.f.}}$ . As both  $g_*^2$  and  $g_{\text{cr}}^2$  depend on the number of flavors, the criticality condition  $g_*^2(N_{f,\text{cr}}) = g_{\text{cr}}^2(N_{f,\text{cr}})$  defines the lower end of the conformal window and thus the critical flavor number, see Sect. II and the left panel of Fig. 3 for an illustration.

For  $g_*^2 > g_{\text{cr}}^2$ , our model (3) is below the conformal window and runs into the broken phase. Slightly below the conformal window, the running coupling  $g^2$  exceeds the critical value while it is in the attractive domain of the IR fixed point  $g_*^2$ . The flow in this fixed-point regime can approximately be described by a  $\beta$  function expanded around the fixed point  $g_*^2$ :

$$\beta_{g^2} \equiv \partial_t g^2 = -\Theta (g^2 - g_*^2) + \mathcal{O}((g^2 - g_*^2)^2). \quad (16)$$

The universal "critical exponent"  $\Theta$  denotes (minus) the first expansion coefficient. We know that  $\Theta < 0$ , since the fixed point is IR attractive, see right panel of Fig. 3. In general, the critical exponent depends on  $N_f$ ,  $\Theta = \Theta(N_f)$ . The solution to Eq. (16) for the running coupling in the fixed-point regime simply reads

$$g^2(k) = g_*^2 - \left(\frac{k}{k_0}\right)^{-\Theta}, \quad (17)$$

where the scale  $k_0$  is implicitly defined by a suitable initial condition and is kept fixed in the following as we keep the UV scale  $\Lambda$  fixed.

The scale  $k_0$  corresponds to a scale where the system is already in the fixed-point regime. For the present fixed-point considerations,  $k_0$  provides for all dimensional scales. However, from the knowledge of the full RG trajectory,  $k_0$  can be related to the initial scale  $\Lambda$ , say the  $\tau$  mass scale in QCD, by RG evolution.

A necessary condition for (chiral) symmetry breaking is that  $g_*^2 > g_{\text{cr}}^2$ . This implies that  $g^2(k)$  exceeds  $g_{\text{cr}}^2$  at some scale  $k_{\text{cr}}$  which is implicitly defined by the criticality condition,  $g_*^2(N_{f,\text{cr}}) = g_{\text{cr}}^2(N_{f,\text{cr}})$ , and therefore

$$k_{\text{cr}} \geq k_{\text{SB}}, \quad (18)$$

where  $k_{\text{SB}}$  is the scale at which the four-fermion coupling  $\lambda$  diverges, see Sect. II. Thus,  $k_{\text{cr}}$  is an upper bound for the symmetry breaking scale  $k_{\text{SB}}$ . From Eq. (17) and the criticality condition  $g^2(k_{\text{cr}}) = g_{\text{cr}}^2$ , we derive an estimate for  $k_{\text{cr}}$  valid in the fixed-point regime

$$k_{\text{cr}} \simeq k_0 (g_*^2 - g_{\text{cr}}^2)^{-\frac{1}{\Theta}}. \quad (19)$$

The scale  $k_{\text{cr}}$  is dynamically generated. Note that  $k_{\text{cr}}/k_0 \rightarrow 0$  for  $g_*^2 \rightarrow g_{\text{cr}}^2$  from above. Due to our scale-fixing procedure, this scale depends on  $N_f$  and  $N_{f,\text{cr}}$  in a

<sup>5</sup> By asymptotic freedom, we refer to the vanishing of the dimensionless renormalized coupling in the UV.

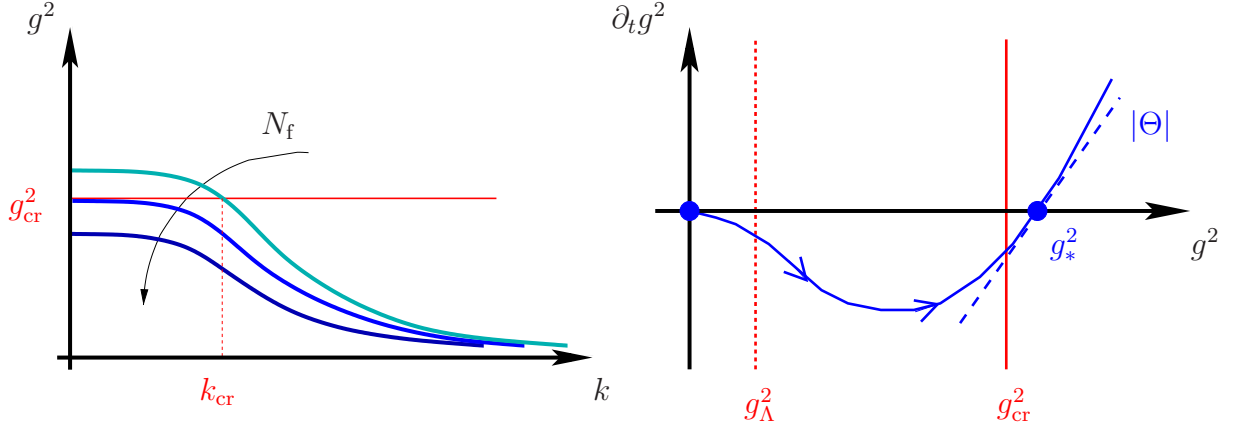


Figure 3: Left panel: illustration of the IR running of the gauge coupling in comparison with the critical value of the gauge coupling  $g_{\text{cr}}^2$ . Below the conformal window,  $N_f < N_{f,\text{cr}}$ ,  $g^2$  exceeds the critical value  $g_{\text{cr}}^2$ , triggering the approach to  $\chi\text{SB}$ . For increasing flavor number, the IR fixed-point value  $g_*^2$  becomes smaller than the critical value, indicating that the theory is inside the conformal window. Right panel: sketch of the  $\beta$  function of the running gauge coupling. The slope of the  $\beta$  function at the IR fixed-point corresponds to minus the critical exponent  $\Theta$ , cf. Eq. (16). The vertical line to the right gives the value of  $g_{\text{cr}}^2$ . The dotted line gives the value of the gauge coupling at the UV scale  $\Lambda$  which we keep fixed for all  $N_f$ . By contrast, the value of  $g_{\text{cr}}^2$  may depend on  $N_f$ . The arrows indicate the direction of the flow towards the infrared.

non-trivial way<sup>6</sup>. Using Eq. (14) and a Taylor expansion of the critical exponent near the quantum phase transition,

$$\Theta(N_f) = \Theta_0 + \Theta_1(N_f - N_{f,\text{cr}}) + \mathcal{O}((N_f - N_{f,\text{cr}})^2), \quad (20)$$

we find the following  $N_f$  dependence of  $k_{\text{cr}}$  for  $N_f \leq N_{f,\text{cr}}$ :

$$k_{\text{cr}} \simeq k_0 |N_{f,\text{cr}} - N_f|^{-\frac{1}{\Theta_0}} \times \left( 1 - \frac{|N_{f,\text{cr}} - N_f|}{\Theta_0} \left( \frac{\alpha_2}{\alpha_1} - \frac{\Theta_1}{\Theta_0} \ln(\alpha_1 |N_{f,\text{cr}} - N_f|) \right) \right) + \dots, \quad (21)$$

where  $\Theta_0 = \Theta(N_{f,\text{cr}})$ . Since  $k_{\text{cr}}$  defines the scale at which the fixed-points in the  $\beta$  function of the four-fermion coupling merge, the existence of a finite  $k_{\text{cr}}$  can be considered as a necessary condition for (chiral) symmetry breaking. Thus, we expect that the scale for a given IR observables  $\mathcal{O}$  for  $N_f \leq N_{f,\text{cr}}$  is set by  $k_{\text{cr}}$ :

$$\mathcal{O} = f_{\mathcal{O}} k_{\text{cr}}^{d_{\mathcal{O}}}, \quad (22)$$

where  $d_{\mathcal{O}}$  is the canonical mass dimension and  $f_{\mathcal{O}}$  depends on  $N_f$  but not on  $N_{f,\text{cr}}$ , see also Eq. (12). However, we would like to stress that  $k_{\text{cr}}$  does not include the full dependence of  $k_{\text{SB}}$  on  $(N_f - N_{f,\text{cr}})$ , i. e.  $k_{\text{cr}}/k_{\text{SB}} \neq \text{const.}$  is still a function of the control parameter, as we shall discuss in the subsequent section.

In Ref. [37, 38, 66] we have implicitly used the existence of a finite  $k_{\text{cr}}$  to estimate the chiral phase transition temperature in QCD as a function of  $N_f$ . For a given value

of  $N_f$  the phase transition temperature is given by the highest temperature for which we still have  $k_{\text{cr}} > 0$ . We have indeed found that  $T_{\text{cr}}$  scales according to Eq. (21):

$$T_{\text{cr}} \sim k_0 |N_{f,\text{cr}} - N_f|^{-\frac{1}{\Theta_0}}. \quad (23)$$

Strictly speaking, this is only an upper bound for the chiral phase transition temperature since it is only sensitive to the emergence of a fermion condensate on intermediate (momentum) scales but insensitive to a fate of the condensate in the deep IR close to  $T_{\text{cr}}$  due to fluctuations of Goldstone modes [75], also known as a local ordering phenomena. Such strong IR fluctuations of the Goldstone modes may yield corrections to the scaling law for the critical temperature given above<sup>7</sup>. Nevertheless, relation (23) is an analytic prediction for the shape (of the upper bound of) the chiral phase boundary in the  $(T, N_f)$  plane.

At vanishing temperature, the analysis of the scaling behavior of IR observables is simplified compared to a scaling analysis at finite temperature since dimensional reduction does not set in in the deep IR enhancing the Goldstone modes. Based on the observed scaling behavior of  $k_{\text{cr}}$  with the number of flavors, we are therefore in a position to derive the  $N_f$  scaling of low-energy observables, such as fermion condensates, at zero temperature.

<sup>6</sup> Note that it is, in principle, possible to adjust the initial value of the coupling at the initial scale such that the scale  $k_{\text{cr}}$  is independent of  $N_f$  and  $N_{f,\text{cr}}$ . As indicated above, we expect that such a scale-fixing procedure would, however, be strongly affected by scheme-dependencies at least in our truncation.

<sup>7</sup> We would naively expect that corrections to Eq. (23) can be only resolved in lattice simulations with very small masses for the pseudo Goldstone modes and on very large lattice sizes, see also Sect. IV.

#### IV. BEYOND MIRANSKY SCALING

Let us now discuss how the symmetry breaking scale  $k_{\text{SB}} \leq k_{\text{cr}}$  depends on  $(N_f - N_{f,\text{cr}})$ . We consider again a Lagrangian of the form (3), and assume that  $N_f \lesssim N_{f,\text{cr}}$ . The crucial new ingredient compared to the derivation of Miransky scaling is the RG flow of the coupling. We also assume that the system has already evolved from the initial UV scale  $\Lambda$  to the scale  $k_{\text{cr}}$  at which the fixed points of the  $\beta$  function of the four-fermion coupling have merged. Sufficiently close to  $N_{f,\text{cr}}$ , the flow of the gauge coupling is governed by the fixed point regime for  $g^2 > g_{\text{cr}}^2$ . The running of the gauge coupling is then given by (cf. Eq. (17))

$$\begin{aligned} g^2(k) &= g_*^2 - (g_*^2 - g_{\text{cr}}^2) \left( \frac{k}{k_{\text{cr}}} \right)^{-\Theta} \\ &= g_*^2 - (\Delta g^2) \left( \frac{k}{k_{\text{cr}}} \right)^{-\Theta}, \end{aligned} \quad (24)$$

where  $\Delta g^2 = g_*^2 - g_{\text{cr}}^2$ . Recall that  $g_*^2 \sim N_f$  and  $\Delta g^2 \sim |N_{f,\text{cr}} - N_f|$ . Plugging Eq. (24) into Eq. (4), we find

$$\begin{aligned} \beta_\lambda &\equiv \partial_t \lambda = \beta_\lambda \Big|_{g_*^2} + \frac{\partial \beta_\lambda}{\partial g^2} \Big|_{g_*^2} (\Delta g^2) \left( \frac{k}{k_{\text{cr}}} \right)^{-\Theta} + \dots \quad (25) \\ &= (d-2)\lambda - a\lambda^2 - b\lambda g_*^2 - c g_*^4 + \frac{\partial \beta_\lambda}{\partial g^2} \Big|_{g_*^2} \left( \frac{k}{k_0} \right)^{-\Theta} + \dots, \end{aligned}$$

where we have used Eq. (19). Recall that  $k \leq k_{\text{cr}} \ll k_0$  and  $\Theta < 0$ . We observe that the zeroth order in  $\Delta g^2$  coincides with the  $\beta_\lambda$  function for which we have found an (implicit) analytic solution for constant  $g^2$  in Sect. II yielding Miransky scaling. We refer to this analytic solution as  $\lambda_{g_*^2}$ . The solution of the  $\beta$  function (25) can then be found by an expansion around the solution  $\lambda_{g_*^2}$ :

$$\begin{aligned} \lambda &= \lambda_{g_*^2} + (\Delta g^2) \delta \lambda + \dots \\ &= \lambda_{g_*^2} + \left( \frac{k_{\text{cr}}}{k_0} \right)^{-\frac{1}{\Theta}} \delta \lambda + \dots \end{aligned} \quad (26)$$

This allows us to systematically compute the scaling behavior for  $N_f \lesssim N_{f,\text{cr}}$ . Since we are interested in the (chiral) symmetry breaking scale  $k_{\text{SB}}$  we have to solve  $1/\lambda(k_{\text{SB}}) = 0$  for  $k_{\text{SB}}$ . In zeroth order the scale  $k_{\text{SB}}$  can be computed along the lines of our analysis in Sect. II. We find

$$\begin{aligned} k_{\text{SB}} &\propto k_{\text{cr}} \theta(N_{f,\text{cr}} - N_f) \exp \left( -\frac{\pi}{2\epsilon \sqrt{\alpha_1 |N_{f,\text{cr}} - N_f|}} \right) \\ &\simeq k_0 \theta(N_{f,\text{cr}} - N_f) |N_{f,\text{cr}} - N_f|^{-\frac{1}{\Theta_0}} \\ &\quad \times \exp \left( -\frac{\pi}{2\epsilon \sqrt{\alpha_1 |N_{f,\text{cr}} - N_f|}} \right), \end{aligned} \quad (27)$$

where we have used Eq. (21) in leading order. Higher order corrections to Eq. (27) can be computed systematically as outlined above and in the previous sections.

Thus, we have found a *universal* correction to the exponential scaling behavior which is uniquely determined by the universal "critical" exponent  $\Theta$ . A similar result has been suggested very recently by Jarvinen and Sannino using a standard rainbow-ladder approach with a constant gauge coupling but a properly adjusted scale [67]. Our RG analysis demonstrates in a simple and systematic way that such a rainbow-ladder approach is indeed justified and yields the correct leading-order scaling behavior.

Let us now turn to the scaling behavior of physical observables. The scale of all low-energy observables is set by  $k_{\text{SB}}$ . In other words,  $k_{\text{SB}}$  represents the UV cutoff of an effective theory at low energies, such as chiral perturbation theory, quark-meson or NJL-type models in case of QCD. At zero temperature we therefore expect that a given IR observable  $\mathcal{O}$  with mass dimension  $d_{\mathcal{O}}$  scales according to

$$\mathcal{O} = f_{\mathcal{O}}(N_f) \theta(N_{f,\text{cr}} - N_f) k_{\text{SB}}^{d_{\mathcal{O}}}, \quad (28)$$

where  $f_{\mathcal{O}}(N_f)$  is a function which depends on  $N_f$  but not on  $N_{f,\text{cr}}$ . As mentioned above,  $f_{\mathcal{O}}(N_f)$  can be in principle systematically computed in QCD using, e. g., chiral perturbation theory or a large- $N_c$  expansion. For instance, in a large- $N_c$  expansion it is straightforward to derive the leading  $N_f$  dependence of the function  $f_{\mathcal{O}}(N_f)$  for the pion decay constant  $f_\pi$ . It reads [66]

$$f_{f_\pi}(N_f) \sim \sqrt{N_f}. \quad (29)$$

The scaling law (28) together with (27) represents one of the main results of this work. It can be used as an ansatz to fit, e. g., data from lattice simulations. This scaling law is remarkable for a number of reasons: first, it relates two universal quantities with each other: quantitative values of observables and the IR critical exponent. Second, it establishes a quantitative connection between the (chiral) phase structure and the IR gauge dynamics ( $\Theta$ ). Third, it is a parameter-free prediction following essentially from scaling arguments. Moreover, it shows that Miransky scaling and power-law scaling are simply two limits of the very same set of RG flows: in the limit  $\Theta \rightarrow \infty$  we find pure Miransky-scaling behavior, while we have pure power-law scaling in the limit  $\Theta \rightarrow 0$ .

At this point, we would like to emphasize once more that the scaling behavior of any IR observable near  $N_{f,\text{cr}}$  depends crucially on the scale-fixing procedure applied in the first place. Still, the universal scaling will always show up at one or the other place and thus cannot be removed, as stressed in Ref. [66]. Our choice to fix the scale at  $m_\tau$  which is large enough not to be affected by chiral-symmetry-breaking is certainly not unique. In principle, the point where to fix the scale can be chosen as a free function of  $N_f$ . In Eq. (17), this would correspond to the choice of an arbitrary function  $k_0 = k_0(N_f)$  for the global scale, which then appears also in the scaling relations (21), (23) and (27). Indeed, an extreme choice would be given by measuring all dimensionful scales in units of a scale induced by chiral symmetry breaking

(such as  $T_{\text{cr}}$  or  $f_\pi$ ). In this case, all chiral observables would jump non-analytically across  $N_f = N_f^{\text{cr}}$ . Nevertheless, the scaling relations would then translate into scaling relations for other non-chiral external scales: e.g., the scale  $k$  at which the running coupling acquires a specific value (say  $\alpha = 0.322$ ) would diverge with  $N_f \rightarrow N_f^{\text{cr}}$  according to  $k \sim |N_f - N_f^{\text{cr}}|^{-\frac{1}{|\Theta_0|}}$ . This point of view can constitute a different way of verifying our scaling relations on the lattice.

Let us conclude this section with a discussion of the importance of the corrections to the exponential scaling behavior due to the running of the gauge coupling. To that end, it is convenient to consider the logarithm of the (chiral) symmetry breaking scale  $k_{\text{SB}}$ ,

$$\ln k_{\text{SB}} = \text{const.} - \frac{1}{\Theta_0} \ln |N_{f,\text{cr}} - N_f| - \frac{\pi}{2\epsilon \sqrt{\alpha_1 |N_{f,\text{cr}} - N_f|}}. \quad (30)$$

This expression can be used to estimate the regime in which the corrections to the exponential scaling become subdominant. For this, we compute the minimum of the function

$$\frac{1}{|\Theta_0|} \ln |N_{f,\text{cr}} - N_f| + \frac{\pi}{2\epsilon \sqrt{\alpha_1 |N_{f,\text{cr}} - N_f|}} \quad (31)$$

with respect to  $|N_{f,\text{cr}} - N_f|$ . In accordance with Eq. (20), we assume  $|N_{f,\text{cr}} - N_f| < 1$  here. From this, we can then estimate that corrections to the exponential scaling behavior are subdominant as long as

$$|N_f - N_{f,\text{cr}}| \lesssim \frac{\pi^2 |\Theta_0|^2}{16\epsilon^2 \alpha_1}, \quad (32)$$

with  $\epsilon$  begin defined in Eq. (11). We observe that corrections to Miransky scaling due to the running of the gauge coupling are small when  $|\Theta_0| \gg 1$  and large when  $|\Theta_0| \ll 1$ . To be more specific, let us consider QCD with many flavors: assuming  $N_{f,\text{cr}} \approx 12$ , we extract  $\Theta_0 \approx 0.4$  from the two-loop  $\beta_{g^2}$  function. From Eq. (32) the region where pure Miransky scaling dominates is then found to be confined to the regime  $|N_f - N_{f,\text{cr}}| \lesssim 0.3$ . Thus, we expect that the exponential scaling behavior is dominantly visible only very close to  $N_{f,\text{cr}}$ . According to this estimate, the  $\Theta$ -dependent universal corrections are therefore more significant in QCD.

In QCD, it appears to be a general feature that  $\Theta_0$  decreases with  $N_{f,\text{cr}}$ . Estimates of  $\Theta_0$  within two- and higher-loop approximations in the  $\overline{\text{MS}}$  scheme are summarized in Fig. 4. Therefore, power-law scaling is more prominent for larger  $N_{f,\text{cr}}$ . In particular, power-law scaling should be visible if theories are probed only for integer values of  $N_f$  as, e.g., on the lattice.

The role of  $|\Theta|$  for the scaling behavior close to  $N_{f,\text{cr}}$  can also be understood by simply looking at the  $\beta_{g^2}$  function of the gauge coupling, see Fig. 3. For  $|\Theta| \gg 1$  the gauge coupling runs very fast into its IR fixed point once it has passed  $g_{\text{cr}}^2$ . Thus, the situation for  $g^2 > g_{\text{cr}}^2$  is as close as possible to the situation studied in Sect. II. The

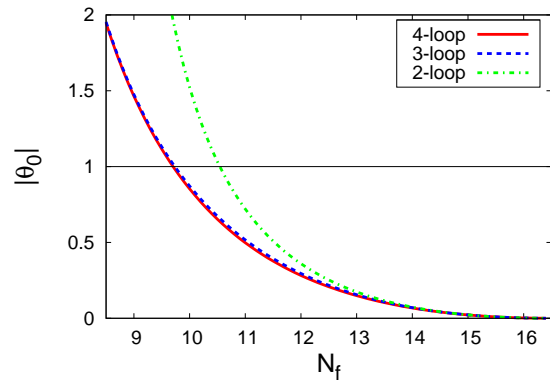


Figure 4: Critical exponent  $\Theta$  of the running gauge coupling at the Caswell-Banks-Zaks fixed point as a function of the number of flavors  $N_f$  as obtained from two-, three- and four-loop perturbation theory in the  $\overline{\text{MS}}$  scheme.

coupling can simply be approximated by a constant. For  $|\Theta| \ll 1$  the gauge coupling runs very slowly (“walks”) into its IR fixed point once it has passed  $g_{\text{cr}}^2$ . This walking behavior for  $g^2 \gtrsim g_{\text{cr}}^2$  then gives rise to sizable corrections to the exponential scaling behavior.

Finally, we would like to discuss the finite-temperature many-flavor phase boundary in QCD. In [37, 38] it was found that the scaling of the phase boundary is consistent with the pure power-law scaling behavior (23). From the above discussion this result is now understandable since the exponential scaling behavior sets in only very close to  $N_{f,\text{cr}}$  for  $N_{f,\text{cr}} \approx 12$  and thus remains invisible in numerical fits over a wider range of  $N_f$ . Of course, power-law scaling behavior for the chiral phase-transition temperature still remains an upper bound even if we took into account the exponential factor in Eq. (28). This is due to the fact that strong fluctuations of Goldstone modes in the IR may yield further corrections and lower the phase transition temperature, see e. g. Ref. [75]. Whether these corrections at finite temperature yield additional corrections to the scaling behavior cannot be answered within the scaling analysis presented in this work. However, it may very well be that such corrections depend only on  $N_f$  but not on  $N_{f,\text{cr}}$ . Nevertheless, we would like to stress that a further investigation of the finite-temperature scaling behavior at the *quantum critical point*,  $N_f = N_{f,\text{cr}}$ , seems worthwhile in QCD since the scaling behavior in  $N_f$  direction may significantly differ from the expected power-law scaling behavior in the temperature direction at fixed  $N_f$ , see [76].

## V. QUANTITATIVE SCALING ANALYSIS IN MANY-FLAVOR QCD

Having derived analytic scaling relations for physical observables in the previous sections, we present results from a numerical study of the scaling behavior in QCD



with many flavors in this section.

### A. Renormalization group setup

Our numerical analysis is based on previous works on strongly-flavored gauge theories in the framework of a functional RG approach using the Wetterich equation [77], for reviews, see [78–87]. In [36] the zero-temperature quantum phase transition of QCD with  $N_c$  colors and  $N_f$  flavors has been computed using the functional RG. The phase diagram at finite temperature as a function of  $N_f$  has first been computed in [37, 38]. We briefly review these results in this section and employ them for our numerical analysis of the scaling behavior.

In [36–38] the RG flow of QCD starting from the microscopic degrees of freedom in terms of quarks and gluons was studied within a covariant derivative expansion. A crucial ingredient for chiral symmetry breaking are the

scale-dependent gluon-induced quark self-interactions of the type included in (3). We note that dynamical quarks influence the RG flow of QCD by qualitatively different mechanisms. First, quark fluctuations directly modify the running of the gauge coupling due to the screening nature of these fluctuations. On the other hand, gluon exchange between quarks induces quark self-interactions which can become relevant operators in the IR as we have already discussed in the previous sections. These two mechanisms strongly influence each other as well. As we have seen, however, it is possible to disentangle the system once we accept that these fluctuations can be associated with different scales in the problem.

From now on we restrict ourselves to  $d = 4$  Euclidean space-time dimensions and work solely in the Landau gauge. In a consistent and systematic operator expansion of the effective action, the lowest nontrivial order is given by [72]

$$\Gamma_k = \int d^4x \left\{ \bar{\psi}(\mathbf{i}\not{\partial} + \bar{g}\not{A})\psi + \frac{1}{2} \left[ \bar{\lambda}_-(V-A) + \bar{\lambda}_+(V+A) + \bar{\lambda}_\sigma(S-P) + \bar{\lambda}_{VA}[2(V-A)^{\text{adj}} + (1/N_c)(V-A)] \right] \right\}. \quad (33)$$

This ansatz for the effective action underlies our non-perturbative RG study. The four-fermion interactions occurring here have been classified according to their color and flavor structure. Color and flavor singlets are

$$(V-A) = (\bar{\psi}\gamma_\mu\psi)^2 + (\bar{\psi}\gamma_\mu\gamma_5\psi)^2, \quad (34)$$

$$(V+A) = (\bar{\psi}\gamma_\mu\psi)^2 - (\bar{\psi}\gamma_\mu\gamma_5\psi)^2, \quad (35)$$

where (fundamental) color  $(i, j, \dots)$  and flavor  $(\chi, \xi, \dots)$  indices are contracted pairwise, e.g.,  $(\bar{\psi}\psi) \equiv (\bar{\psi}_i^\chi \psi_i^\chi)$ . The remaining operators have non-singlet color or flavor structure,

$$\begin{aligned} (S-P) &= (\bar{\psi}^\chi \psi^\xi)^2 - (\bar{\psi}^\chi \gamma_5 \psi^\xi)^2 \equiv (\bar{\psi}_i^\chi \psi_i^\xi)^2 - (\bar{\psi}_i^\chi \gamma_5 \psi_i^\xi)^2, \\ (V-A)^{\text{adj}} &= (\bar{\psi}\gamma_\mu T^a \psi)^2 + (\bar{\psi}\gamma_\mu \gamma_5 T^a \psi)^2, \end{aligned} \quad (36)$$

where  $(\bar{\psi}^\chi \psi^\xi)^2 \equiv \bar{\psi}^\chi \psi^\xi \bar{\psi}^\xi \psi^\chi$ , etc., and  $(T^a)_{ij}$  denote the generators of the gauge group in the fundamental representation.

We stress that the set of fermionic self-interactions introduced in Eq. (33) forms a complete basis. This means that any other pointlike four-fermion interaction which is invariant under  $SU(N_c)$  gauge symmetry and  $SU(N_f)_L \times SU(N_f)_R$  flavor symmetry can be related to those in Eq. (33) by means of Fierz transformations. In our numerical analysis, we neglect  $U_A(1)$ -violating inter-

actions induced by topologically non-trivial gauge configurations, since we expect them to become relevant only inside the  $\chi$ SB regime or for small  $N_f$ . In addition, the lowest-order  $U_A(1)$ -violating term schematically is  $\sim (\bar{\psi}\psi)^{N_f}$ . Thus, larger  $N_f$  correspond to larger RG “irrelevance” by naive power-counting. Moreover, interactions of the type  $\sim (\bar{\psi}\psi)^{N_f}$  for  $N_f > 3$  do not contribute directly to the flow of the four-fermion interactions due to the one-loop structure of the underlying RG equation for the effective action.

As a severe approximation, we drop any nontrivial momentum dependencies of the  $\bar{\lambda}$ ’s and study these couplings in the point-like limit  $\bar{\lambda}(|p_i| \ll k)$  in our scaling analysis. Therefore our ansatz for the effective action does not allow us to study QCD properties in the chirally broken regime, since, e. g., mesons manifest themselves as momentum singularities in the  $\bar{\lambda}$ ’s. Nonetheless, our point-like approximation can be reasonable in the chirally symmetric regime. This has been indeed shown in [36], where the regularization-scheme independence of universal quantities has been found to hold remarkably well in the point-like limit.

Using the truncated effective action (33), we obtain the following  $\beta$  functions for the dimensionless couplings  $\lambda_i = \bar{\lambda}_i/k^2$  (see [36, 72]):

$$\begin{aligned} \partial_t \lambda_- = & 2\lambda_- - 4v_4 l_{1,1}^{(\text{FB}),4} \left[ \frac{3}{N_c} g^2 \lambda_- - 3g^2 \lambda_{\text{VA}} \right] - \frac{1}{8} v_4 l_{1,2}^{(\text{FB}),4} \left[ \frac{12 + 9N_c^2}{N_c^2} g^4 \right] \\ & - 8v_4 l_1^{(\text{F}),4} \left\{ -N_f N_c (\lambda_-^2 + \lambda_+^2) + \lambda_-^2 - 2(N_c + N_f) \lambda_- \lambda_{\text{VA}} + N_f \lambda_+ \lambda_\sigma + 2\lambda_{\text{VA}}^2 \right\}, \end{aligned} \quad (37)$$

$$\begin{aligned} \partial_t \lambda_+ = & 2\lambda_+ - 4v_4 l_{1,1}^{(\text{FB}),4} \left[ -\frac{3}{N_c} g^2 \lambda_+ \right] - \frac{1}{8} v_4 l_{1,2}^{(\text{FB}),4} \left[ -\frac{12 + 3N_c^2}{N_c^2} g^4 \right] \\ & - 8v_4 l_1^{(\text{F}),4} \left\{ -3\lambda_+^2 - 2N_c N_f \lambda_- \lambda_+ - 2\lambda_+ (\lambda_- + (N_c + N_f) \lambda_{\text{VA}}) + N_f \lambda_- \lambda_\sigma + \lambda_{\text{VA}} \lambda_\sigma + \frac{1}{4} \lambda_\sigma^2 \right\}, \end{aligned} \quad (38)$$

$$\begin{aligned} \partial_t \lambda_\sigma = & 2\lambda_\sigma - 4v_4 l_{1,1}^{(\text{FB}),4} [6C_2(N_c) g^2 \lambda_\sigma - 6g^2 \lambda_+] - \frac{1}{4} v_4 l_{1,2}^{(\text{FB}),4} \left[ -\frac{24 - 9N_c^2}{N_c} g^4 \right] \\ & - 8v_4 l_1^{(\text{F}),4} \left\{ 2N_c \lambda_\sigma^2 - 2\lambda_- \lambda_\sigma - 2N_f \lambda_\sigma \lambda_{\text{VA}} - 6\lambda_+ \lambda_\sigma \right\}, \end{aligned} \quad (39)$$

$$\begin{aligned} \partial_t \lambda_{\text{VA}} = & 2\lambda_{\text{VA}} - 4v_4 l_{1,1}^{(\text{FB}),4} \left[ \frac{3}{N_c} g^2 \lambda_{\text{VA}} - 3g^2 \lambda_- \right] - \frac{1}{8} v_4 l_{1,2}^{(\text{FB}),4} \left[ -\frac{24 - 3N_c^2}{N_c} g^4 \right] \\ & - 8v_4 l_1^{(\text{F}),4} \left\{ -(N_c + N_f) \lambda_{\text{VA}}^2 + 4\lambda_- \lambda_{\text{VA}} - \frac{1}{4} N_f \lambda_\sigma^2 \right\}. \end{aligned} \quad (40)$$

Here,  $C_2(N_c) = (N_c^2 - 1)/(2N_c)$  is a Casimir operator of the gauge group, and  $v_4 = 1/(32\pi^2)$ . The regularization-scheme dependence of the RG flow equations is controlled by (dimensionless) threshold functions  $l$  which arise from Feynman diagrams and incorporate fermionic and/or bosonic fields [88]. For the optimized regulator [89–91], we find

$$l_1^{(\text{F}),4} = \frac{1}{2}, \quad l_{1,1}^{(\text{FB}),4} = 1 - \frac{\eta_A}{6}, \quad l_{1,2}^{(\text{FB}),4} = \frac{3}{2} - \frac{\eta_A}{6}. \quad (41)$$

In our numerical analysis, we have dropped contributions from the anomalous dimensions of the fermions and the gauge coupling  $\eta_A = \beta_{g^2}/g^2$ . While the first one is proportional to the gauge-fixing parameter and vanishes identical in the Landau gauge in the chirally symmetric regime [72], we have found by a comparison of our numerical results with those from [36] that the contributions  $\propto \eta_A$  in the threshold function do not strongly affect our result for  $N_{f,\text{cr}}$ . In fact, we have  $\eta_A \rightarrow 0$  for  $N_f \rightarrow N_f^{\text{a.f.}}$  and  $g^2 < g_*^2$ . Moreover, we find for  $g^2 < g_*^2$  that  $|\eta_A^{2\text{-loop}}| \lesssim 1$  for  $N_f \gtrsim 11$  and  $|\eta_A^{4\text{-loop}}| \lesssim 0.5$  for  $N_f \gtrsim 8$ . In total, this may lead to quantitative corrections at most on the percent level.

Let us now discuss the running of the gauge coupling. Even though the running coupling has been computed within the functional RG approach [37, 38, 92–94], we employ for simplicity the two- and four-loop result obtained in the  $\overline{\text{MS}}$  scheme [95, 96], as our results show a satisfactory convergence in the strongly flavored regime. We will often restrict ourselves to the two-loop case, as it already shows all qualitative features and can be dealt

with analytically. The analytic expression for the two-loop  $\beta_{g^2}$  function reads explicitly:

$$\partial_t g^2 = - \left( \beta_0 + \beta_1 \left( \frac{g^2}{16\pi^2} \right) + \dots \right) \frac{g^2}{8\pi^2}, \quad (42)$$

with

$$\beta_0 = \frac{11}{3} N_c - \frac{2}{3} N_f, \quad \beta_1 = \frac{34N_c^3 + 3N_f - 13N_c^2 N_f}{3N_c}. \quad (43)$$

Note that the chosen regularization scheme in the matter sector and the  $\overline{\text{MS}}$  scheme do not coincide. This inconsistency results in an error for our estimate for the critical number of quark flavors. Since we are rather interested in the scaling behavior which is related to the universal critical exponent  $\Theta$ , our results are only influenced indirectly by this approximation<sup>8</sup>. Due to this scheme dependence, the results using the four-loop running may not necessarily be considered as a more precise calculation. Instead, the difference between two-loop and four-loop  $\overline{\text{MS}}$  results should be viewed as an estimate of the dependence of our results on the quantitative details of the running gauge sector.

A comment on contributions to the running of the gauge coupling induced by the presence of the quark self-interactions  $\lambda_i$  is in order here: To render the RG

<sup>8</sup> Of course, the actual value of  $\Theta_0 = \Theta(N_{f,\text{cr}})$  depends on the actual value of  $N_{f,\text{cr}}$  which itself, as a universal quantity, depends on the difference of the scheme-dependent quantities  $g_{\text{cr}}^2$  and  $g_*^2$ .

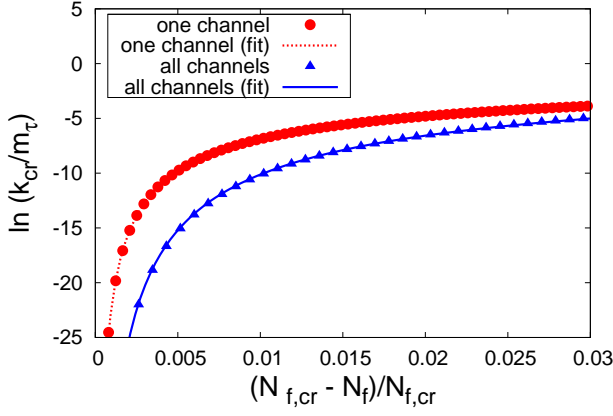


Figure 5: Logarithm of the (chiral) symmetry-breaking scale  $\ln(k_{SB}/m_\tau)$  as a function of  $(N_{f,cr} - N_f)/N_{f,cr}$  for an  $N_f$ -dependent but scale-independent, i.e. constant gauge coupling. The corresponding fits are given in Eq. (52).

flow gauge invariant we have to take regulator-dependent Ward-Takahashi identities into account [92, 97]. In the present case, these symmetry constraints yield contributions to the running of the gauge coupling which depend on the quark self-interactions. However, these contributions are proportional to the  $\beta$  functions of the four-fermion couplings, as has been pointed out in Ref. [36, 72]. Therefore, these contributions vanish as long as the four-fermion couplings are at their fixed points, i. e. as long as  $g^2 \leq g_{cr}^2$ . Thus, we expect that these contributions do not alter the scaling-law (27) in leading order<sup>9</sup>. In particular, the power-law behavior is unaffected by these corrections arising due to symmetry constraints. In the present approximation, we ignore these corrections in our numerical analysis.

### B. Miransky-type scaling

Let us start with a numerical analysis of many-flavor QCD with a constant gauge coupling:

$$\partial_t g^2 = 0.$$

As discussed above, the gauge coupling can then be considered as an "external"  $N_f$ -dependent parameter of the

theory. For our numerical study we choose the fixed-point value of the gauge-coupling at the two-loop level:

$$g_{*,2-loop}^2(N_f) = \frac{16(11N_c^2 - 2N_cN_f)\pi^2}{13N_c^2N_f - 34N_c^3 - 3N_f}. \quad (44)$$

In the matter sector we employ two different truncations to which we refer as *one-channel* and *all-channels* approximation. The latter one is Fierz complete. In the all-channels approximation we take into account the full set of flow equations (37)-(40), while we only take into account the RG flow of the scalar-pseudoscalar channel  $\lambda_\sigma$  in the one-channel approximation and set all other four-fermion couplings to zero:

$$\partial_t \lambda_\sigma = 2\lambda_\sigma - a_\sigma \lambda_\sigma^2 - b_\sigma \lambda_\sigma g^2 - c_\sigma g^4, \quad (45)$$

with

$$\begin{aligned} a_\sigma &= \frac{N_c}{4\pi^2}, & b_\sigma &= \frac{3}{4\pi^2} C_2(N_c), \\ c_\sigma &= \frac{3}{256\pi^2} \left( \frac{9N_c^2 - 24}{N_c} \right). \end{aligned} \quad (46)$$

Here, we have adopted the conventions of Sect. II for the coefficients  $a, b, c$ .

Now we can compute the critical values of the gauge coupling in the one- and in the all-channels approximation. In the one-channel approximation we find

$$g_{cr,one}^2 = \frac{32\pi^2 (2N_c^3 - 2N_c - \sqrt{3N_c^6 - 8N_c^4})}{3(4 + N_c^4)} \Big|_{(N_c=3)} \approx 10.86, \quad (47)$$

which does not depend on  $N_f$ . In the all-channels approximation the critical value has to be computed numerically. As found in [36], the resulting critical value  $g_{cr,all}^2$  of the gauge coupling then depends on  $N_f$ ; for a given number of colors,  $g_{cr,all}^2$  decreases weakly with increasing  $N_f$ .

The fixed-point value  $g_{*,2-loop}^2$  together with the critical value of the gauge coupling can be used to estimate the critical number of quark flavors above which there is no chiral symmetry breaking in the IR. In agreement with the results given in Ref. [36], we find

$$N_{f,cr}^{one} = \frac{169N_c^6 - 136N_c^4 + 132N_c^2 - 68\sqrt{N_c^4(3N_c^2 - 8)}N_c^3}{58N_c^5 - 64N_c^3 - 26\sqrt{N_c^4(3N_c^2 - 8)}N_c^2 + 6\sqrt{N_c^4(3N_c^2 - 8)} + 36N_c} \Big|_{(N_c=3)} \approx 11.7, \quad (48)$$

for the one-channel approximation and

$$N_{f,cr}^{all} \approx 11.9 \quad (49)$$

for the all-channels approximation. We may use our estimate for  $N_{f,cr}$  from the one-channel approximation to

estimate  $N_{f,cr}$  in the limit  $N_c \rightarrow \infty$ :

$$\frac{N_{f,cr}^{one}}{N_c} = \frac{68\sqrt{3} - 169}{2(13\sqrt{3} - 29)} \approx 3.95. \quad (50)$$

Our results for  $N_{f,cr}$  are in accordance with the results from Dyson-Schwinger equations in the rainbow-ladder approximation, see e. g. [6, 32, 73] as well as with those from current lattice simulations [44–57].

Let us now study the dependence of the symmetry breaking scale  $k_{SB}$  on  $N_f$  for the specific case  $N_c = 3$ . In Fig. 5 we show our results for  $\ln(k_{SB}/\Lambda)$  as function of  $(N_{f,cr} - N_f)/N_f$  as obtained from the one-channel (dots) and from the all-channels (triangles) approximation using  $g_{*,2-loop}^2$  as a fixed input parameter. As initial conditions for the  $\lambda_i$ 's for a given  $g_{*,2-loop}^2(N_f)$  we have used the solution of the coupled set of linear equations

$$\frac{\partial(\partial_t \lambda_i)}{\partial \lambda_i} = 0, \quad (51)$$

where  $i \in \{+, -, \sigma, VA\}$ . This corresponds to starting the flow at the maxima (extrema) of the parabolas.

We observe that for a given  $N_f$  the symmetry breaking scale  $k_{SB}$  is smaller in the all-channels approximation compared to the one-channel approximation. The fits to the data points are also shown in Fig. 5. In agreement with our analytic results we find:

$$\begin{aligned} \ln k_{SB}^{one} &\approx \text{const.} - \frac{2.481}{|N_{f,cr} - N_f|^{0.494}}, \\ \ln k_{SB}^{all} &\approx \text{const.} - \frac{3.932}{|N_{f,cr} - N_f|^{0.516}}. \end{aligned} \quad (52)$$

Thus, we clearly observe the expected exponential scaling behavior in the one-channel and in the all-channels approximation for  $N_f \rightarrow N_{f,cr}$ .

The result from the one-channel approximation is in reasonable agreement with the analytic leading-order (LO) result found in Sect. II:

$$\begin{aligned} \ln k_{SB}^{LO} &= \text{const.} - \frac{\pi}{2\epsilon\sqrt{|\alpha_1||N_{f,cr} - N_f|}} \\ &\approx \text{const.} - \frac{2.386}{\sqrt{|N_{f,cr} - N_f|}}. \end{aligned} \quad (53)$$

Note that  $|\alpha_2/\alpha_1| \approx 0.273$ . Differences to the numerical results are due to numerical errors of the fit and higher-order corrections which we have derived in Sect. II.

### C. Power-law scaling and beyond

Let us now take into account the (momentum) scale-dependence of the running gauge coupling. In order to compare the theories with different flavor numbers we fix the scales by keeping the running coupling at the  $\tau$ -mass scale  $\Lambda = m_\tau$  fixed to  $\alpha(m_\tau) \approx 0.322$ . Since we apply the truncation (33) to QCD, we do not consider the

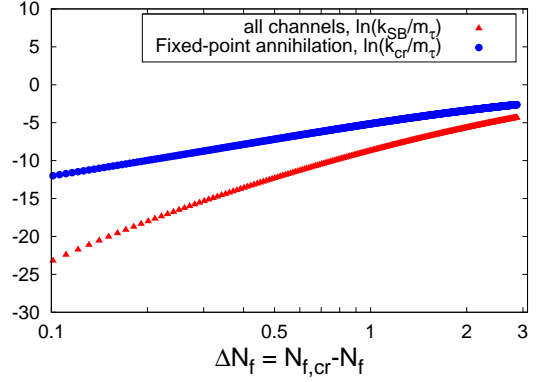


Figure 6:  $N_f$  dependence of  $k_{cr}$  and  $k_{SB}$  as obtained from a study with a running coupling in the two-loop approximation. The criticality scale  $k_{cr}$  (blue circles) is dominated by power-law scaling (straight line with slope  $\sim |\Theta_0|^{-1}$  in this double-log plot), and clearly serves as an upper bound for the symmetry breaking scale  $k_{SB}$  (red triangles), being a superposition of power-law and Miransky scaling. If the theories are probed at integer  $N_f$ , i.e.,  $\Delta N_f \gtrsim \mathcal{O}(1)$ , the contribution due to Miransky scaling may not be visible. A pure powerlaw fit to chiral observables  $\sim k_{SB}$ , may however overestimate the critical exponent  $\Theta_0$ .

four-fermion couplings  $\bar{\lambda}$  as independent external parameters as, e.g., in Nambu–Jona-Lasinio-type models. More precisely, we impose the boundary condition  $\bar{\lambda}_i \rightarrow 0$  for  $k \rightarrow \infty$  which guarantees that the  $\bar{\lambda}$ 's at finite  $k$  are solely generated by quark-gluon dynamics, e.g., by 1PI “box” diagrams with 2-gluon exchange, cf. Fig. 1(c).

In Fig. 6 and Fig. 7 we show our results for the  $N_f$  dependence of the scales  $k_{cr}$  and  $k_{SB}$  as obtained from a study with a running gauge coupling in the two-loop and the four-loop approximation, respectively. Note that  $N_{f,cr}$  becomes smaller when we employ the running coupling in the four-loop approximation. We find

$$N_{f,cr}^{4-loop} \approx 10.0 \quad (54)$$

in the all-channels approximation and  $N_{f,cr}^{4-loop} \approx 9.8$  in the one-channel approximation, in agreement with Ref. [36].

The data points can be fitted to our analytic results for the scaling behavior of  $k_{SB}$  and  $k_{cr}$ . For the all-channels approximation, we find

$$\ln k_{cr}^{2-loop} \approx \text{const.} + 2.566 |N_f - N_{f,cr}|, \quad (55)$$

$$\begin{aligned} \ln k_{SB}^{2-loop} &\approx \text{const.} - \frac{3.401}{|N_f - N_{f,cr}|^{0.54}} \\ &\quad + 2.540 \ln |N_f - N_{f,cr}|, \end{aligned} \quad (56)$$

and

$$\ln k_{cr}^{4-loop} \approx \text{const.} + 1.180 |N_f - N_{f,cr}|, \quad (57)$$

$$\begin{aligned} \ln k_{SB}^{4-loop} &\approx \text{const.} - \frac{5.196}{|N_f - N_{f,cr}|^{0.52}} \\ &\quad + 1.171 \ln |N_f - N_{f,cr}|. \end{aligned} \quad (58)$$



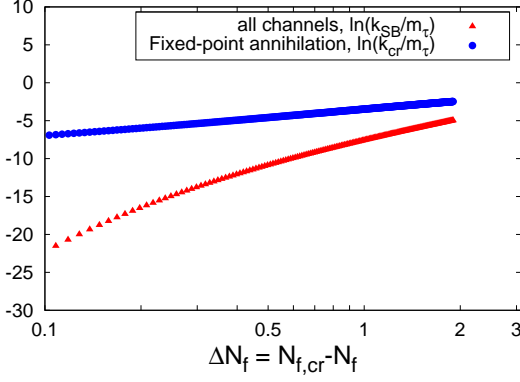


Figure 7:  $N_f$  dependence of  $k_{cr}$  and  $k_{SB}$  as obtained from a study with a running gauge coupling in the four-loop approximation. The contributions due to Miransky scaling, roughly parameterized by the difference between  $k_{cr}$  (blue circles) and  $k_{SB}$  (red triangles), extend to larger values of  $\Delta N_f = N_{f,cr} - N_f$ , as the estimate for the critical exponent  $\Theta_0 = \Theta(N_{f,cr})$  at four loop is larger than at two-loop. In this perturbative estimate for the running coupling, the curves cannot be extended to larger values of  $\Delta N_f$ , see text.

Thus, the fits are in reasonable agreement with our analytic predictions. For the multi-parameter fits (56) and (58), we have fixed the coefficient of the  $\ln$ -term which is the inverse critical exponent  $\Theta_0 = \Theta(N_{f,cr})$ . It should be stressed that the predicted values for the critical exponent  $\Theta(N_{f,cr})$  are substantially different for the running coupling in the two- and four-loop approximation (cf. Fig 4),

$$\begin{aligned} \frac{1}{|\Theta(N_{f,cr})|} &\approx 2.540 \quad (\text{two-loop}), \\ \frac{1}{|\Theta(N_{f,cr})|} &\approx 1.171 \quad (\text{four-loop}). \end{aligned} \quad (59)$$

In Fig. 6 and Fig. 7 we observe that the critical exponent  $\Theta$  clearly influences the scaling behavior close to the quantum critical point  $N_{f,cr}$ . In agreement with our analytic findings, the size of the regime with exponential scaling increases with increasing critical exponent  $\Theta$ . Using Eq. (32) we can give a quantitative estimate for the size of the regime in which the exponential scaling behavior dominates. For the one-channel approximation, cf. Eq. (48), we find:

$$\Delta N_f := |N_f - N_{f,cr}| \lesssim 0.3 \quad (\text{two-loop}, N_{f,cr} \approx 11.7). \quad (60)$$

Using a running coupling in four-loop order ( $N_{f,cr} \approx 9.8$ ) the size of this Miransky scaling regime can be estimated to be larger than one flavor. This is in agreement with our numerical results, see Figs. 6 and 7. With this perturbative estimate for the running coupling, however, the curves in Figs. 6 and 7 cannot be extended to larger values of  $\Delta N_f = N_{f,cr} - N_f$ . For instance, in the four-loop case, we have  $N_{f,cr} \simeq 9.8$  on the one hand. On the other hand, the Caswell-Banks-Zaks fixed point vanishes for

$N_f \lesssim 8$ . Our RG arguments based on expansions about an IR fixed point hence only extend to  $\Delta N_{f,max} \simeq 1.8$ , cf. Fig. 7. In nonperturbative functional studies where an IR fixed point appears to exist already in the pure gauge sector and thus also at lower  $N_f$  [37, 38, 98–105], no restriction on  $\Delta N_f$  arises.

To summarize: since  $N_{f,cr} \gtrsim 9$  in current lattice simulations [44–57], we expect that the pure exponential scaling behavior is difficult to resolve and the corrections due to the running of the gauge coupling ( $\Theta$ ) might be more relevant for lattice simulations. From the viewpoint of such simulations, one might be interested in keeping the power of the “Miransky” term fixed to 1/2 and use the scaling law to fit  $N_{f,cr}$  and the critical exponent  $\Theta_0 = \Theta(N_{f,cr})$ .

To illustrate the influence of the critical exponent  $\Theta$  we have also computed the scaling behavior of the scales  $k_{cr}$  and  $k_{SB}$  using a model for the running gauge coupling. This model is inspired by the two-loop approximation modified by an artificial higher-order term. The latter is constructed such that the critical exponent  $\Theta$  can be changed by hand, still leaving the two-loop fixed point unaffected:

$$\partial_t g^2 \equiv \beta_{g^2} = \beta_{g^2}^{2\text{-loop}} + \phi g^6 (g^2 - g_{*,2\text{-loop}}^2), \quad (61)$$

where the parameter  $\phi$  allows us to change  $\Theta$  without changing  $N_{f,cr}$ . In Fig. 8 we present our results  $k_{SB}$  and  $k_{cr}$  for  $\phi = 0.003$  (i. e.  $|\Theta(N_{f,cr})| \approx 4.3$ ) in the left panel and for  $\phi = -0.0001$  (i. e.  $|\Theta(N_{f,cr})| \approx 0.3$ ) in the right panel. The results clearly confirm that the size of the exponential-scaling regime depends strongly on  $\Theta$ .

## VI. CONCLUSIONS

In this work we have analyzed how physical observables in asymptotically free gauge theories, such as QCD or QED<sub>3</sub>, scale when the number of flavors is varied. When the number  $N_f$  of fermion flavors in such theories is increased, a regime may open up along the  $N_f$  axis in which the theory is asymptotically free but remains chirally symmetric in the infrared. This gives rise to the existence of a quantum critical point on the  $N_f$  axis. The exact determination of the location of this quantum critical point in QCD as well as in QED<sub>3</sub> is currently a very active frontier in theoretical physics.

Even though we have presented estimates for  $N_{f,cr}$  as obtained from a functional RG approach, see also [36, 38], the focus of this work is on the actual scaling behavior of physical observables close to the quantum critical point. This scaling behavior of observables such as the fermion condensate close to  $N_{f,cr}$  is not only interesting in its own right but may also help to guide future lattice simulations in this field.

Ignoring the running of the gauge coupling, it has long been known that physical observables obey Miransky scaling, i.e., an exponential scaling law close to the quantum critical point [27, 59, 62–64]. In more recent

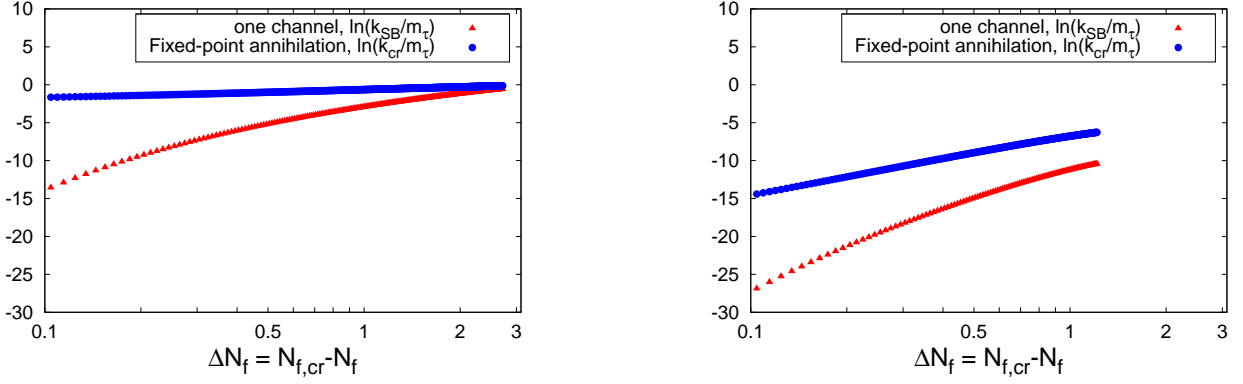


Figure 8:  $N_f$  dependence of  $k_{cr}$  (blue circles) and  $k_{SB}$  (red triangles) as obtained from a study with a model for the running gauge coupling, cf. Eq. (61), that allows to tune the critical exponent  $\Theta$  by hand. We show the results for  $\Theta_0 = |\Theta(N_{f,cr})| \approx 4.3$  (left panel) and  $|\Theta_0| \approx 0.3$  (right panel). Contributions due to Miransky scaling are visible as deviations from a straight-line behavior (power law) in this double-log plot. These results confirm our estimate that the Miransky-scaling window is larger for larger  $|\Theta_0|$  (left panel), whereas power-law scaling dominates for small  $|\Theta_0|$  (right panel).

studies [38, 66] we have shown that an upper bound for the scaling behavior of, e. g. the chiral phase transition temperature, can be derived from an analysis of the fixed-point structure in the matter sector. In combination with the running of the gauge coupling in its fixed-point regime, the upper bound for physical observables then scales according to a power law. The associated critical exponent is related to the universal critical exponent  $\Theta$  at the IR fixed-point of the gauge coupling, see Eq. (21).

From another viewpoint, we have shown that Miransky scaling close to  $N_{f,cr}$  receives universal power-law corrections, which are uniquely determined by the critical exponent at the IR fixed-point of the gauge coupling. Both scaling laws follow from one and the same set of RG flow equations and can be considered as two different limits of a general scaling law: pure exponential Miransky scaling arises in the limit of large  $\Theta \rightarrow \infty$ , whereas power-law scaling becomes more prominent at small  $\Theta \rightarrow 0$ . Quantitatively, we have estimated the size of the regime with almost pure exponential scaling in strongly-flavored QCD and found it to be small,  $|N_{f,cr} - N_f| \lesssim 0.3$  for  $N_{f,cr} \approx 11.7$ . Outside this regime the scaling behavior of physical observables is controlled by the critical exponent  $\Theta$ . Our numerical analysis of scaling in many-flavor QCD based on functional RG methods is indeed in agreement with these analytic findings.

Finally we would like to add that the scaling behavior close to the quantum critical point can be contaminated by the scale-fixing procedure. As also argued in [66], a comparison of theories with different  $N_f$  is not unique

for non-conformal theories but indeed requires a specific choice of a dimensionful scale. This scale is used as a ruler for the different theories. In the present work, we have fixed the scales by keeping the gauge coupling fixed to the same value for all  $N_f$  at an initial mid-momentum scale, e. g. the  $\tau$  mass scale in QCD. Alternatively, theories with different  $N_f$  can be fixed by keeping an IR observable characteristic for the ordered phase for all  $N_f$  fixed, say the pion decay constant  $f_\pi$  or  $T_{cr}$  in QCD. However, the behavior of physical observables at the quantum critical point is then discontinuous.

In any case, the scaling relation (28) is a parameter-free testable prediction for the behavior of physical observables near the quantum critical point. On the one hand, it might be tested directly by lattice simulations. On the other hand, our prediction might also be helpful to guide future lattice simulations of strongly-flavored gauge theories.

### Acknowledgments

The authors thank D. D. Dietrich, J. M. Pawłowski and F. Sannino for useful discussions and acknowledge support by the DFG under grants Gi 328/1-4, Gi 328/5-1 (Heisenberg program), FOR 723 and GRK 1523/1 and by the Helmholtz-University Young Investigator Grant No. VH-NG-332 and by the Helmholtz International Center for FAIR within the LOEWE program of the State of Hesse.

- 
- [1] S. Weinberg, Phys. Rev. **D19**, 1277 (1979).
  - [2] B. Holdom, Phys. Rev. **D24**, 1441 (1981).
  - [3] D. K. Hong, S. D. H. Hsu, and F. Sannino, Phys. Lett.

- B597**, 89 (2004), hep-ph/0406200.
- [4] F. Sannino and K. Tuominen, Phys. Rev. **D71**, 051901 (2005), hep-ph/0405209.

- [5] D. D. Dietrich, F. Sannino, and K. Tuominen, Phys. Rev. **D72**, 055001 (2005), hep-ph/0505059.
- [6] D. D. Dietrich and F. Sannino, Phys. Rev. **D75**, 085018 (2007), hep-ph/0611341.
- [7] T. A. Ryttov and F. Sannino, Phys. Rev. **D76**, 105004 (2007), 0707.3166.
- [8] O. Antipin and K. Tuominen, Phys. Rev. **D81**, 076011 (2010), 0909.4879.
- [9] F. Sannino, Acta Phys. Polon. **B40**, 3533 (2009), 0911.0931.
- [10] W. E. Caswell, Phys. Rev. Lett. **33**, 244 (1974).
- [11] T. Banks and A. Zaks, Nucl. Phys. **B196**, 189 (1982).
- [12] R. D. Pisarski, Phys. Rev. **D29**, 2423 (1984).
- [13] T. W. Appelquist, M. J. Bowick, D. Karabali, and L. C. R. Wijewardhana, Phys. Rev. **D33**, 3704 (1986).
- [14] T. Appelquist, D. Nash, and L. C. R. Wijewardhana, Phys. Rev. Lett. **60**, 2575 (1988).
- [15] D. Atkinson, P. W. Johnson, and P. Maris, Phys. Rev. **D42**, 602 (1990).
- [16] M. R. Pennington and D. Walsh, Phys. Lett. **B253**, 246 (1991).
- [17] D. C. Curtis, M. R. Pennington, and D. Walsh, Phys. Lett. **B295**, 313 (1992).
- [18] C. J. Burden and C. D. Roberts, Phys. Rev. **D44**, 540 (1991).
- [19] P. Maris, Phys. Rev. **D52**, 6087 (1995), hep-ph/9508323.
- [20] V. P. Gusynin, A. H. Hams, and M. Reenders, Phys. Rev. **D53**, 2227 (1996), hep-ph/9509380.
- [21] P. Maris, Phys. Rev. **D54**, 4049 (1996), hep-ph/9606214.
- [22] C. S. Fischer, R. Alkofer, T. Dahm, and P. Maris, Phys. Rev. **D70**, 073007 (2004), hep-ph/0407104.
- [23] E. Dagotto, A. Kocic, and J. B. Kogut, Nucl. Phys. **B334**, 279 (1990).
- [24] S. Hands and J. B. Kogut, Nucl. Phys. **B335**, 455 (1990).
- [25] S. J. Hands, J. B. Kogut, and C. G. Strouthos, Nucl. Phys. **B645**, 321 (2002), hep-lat/0208030.
- [26] S. J. Hands, J. B. Kogut, L. Scorzato, and C. G. Strouthos, Phys. Rev. **B70**, 104501 (2004), hep-lat/0404013.
- [27] V. A. Miransky and K. Yamawaki, Phys. Rev. **D55**, 5051 (1997), hep-th/9611142.
- [28] T. Appelquist, J. Terning, and L. C. R. Wijewardhana, Phys. Rev. Lett. **77**, 1214 (1996), hep-ph/9602385.
- [29] T. Appelquist and S. B. Selipsky, Phys. Lett. **B400**, 364 (1997), hep-ph/9702404.
- [30] T. Schafer and E. V. Shuryak, Rev. Mod. Phys. **70**, 323 (1998), hep-ph/9610451.
- [31] M. Velkovsky and E. V. Shuryak, Phys. Lett. **B437**, 398 (1998), hep-ph/9703345.
- [32] T. Appelquist, A. Ratnaweera, J. Terning, and L. C. R. Wijewardhana, Phys. Rev. **D58**, 105017 (1998), hep-ph/9806472.
- [33] M. Harada and K. Yamawaki, Phys. Rev. Lett. **86**, 757 (2001), hep-ph/0010207.
- [34] F. Sannino and J. Schechter, Phys. Rev. **D60**, 056004 (1999), hep-ph/9903359.
- [35] M. Harada, M. Kurachi, and K. Yamawaki, Phys. Rev. **D68**, 076001 (2003), hep-ph/0305018.
- [36] H. Gies and J. Jaeckel, Eur. Phys. J. **C46**, 433 (2006), hep-ph/0507171.
- [37] J. Braun and H. Gies, Phys. Lett. **B645**, 53 (2007), hep-ph/0512085.
- [38] J. Braun and H. Gies, JHEP **06**, 024 (2006), hep-ph/0602226.
- [39] H. Terao and A. Tsuchiya (2007), 0704.3659.
- [40] E. Poppitz and M. Unsal, JHEP **09**, 050 (2009), 0906.5156.
- [41] A. Armoni, Nucl. Phys. **B826**, 328 (2010), 0907.4091.
- [42] F. Sannino, Phys. Rev. **D80**, 065011 (2009), 0907.1364.
- [43] F. Sannino, Nucl. Phys. **B830**, 179 (2010), 0909.4584.
- [44] J. B. Kogut et al., Phys. Rev. Lett. **48**, 1140 (1982).
- [45] R. V. Gavai, Nucl. Phys. **B269**, 530 (1986).
- [46] M. Fukugita, S. Ohta, and A. Ukawa, Phys. Rev. Lett. **60**, 178 (1988).
- [47] F. R. Brown et al., Phys. Rev. **D46**, 5655 (1992), hep-lat/9206001.
- [48] P. H. Damgaard, U. M. Heller, A. Krasnitz, and P. Olesen, Phys. Lett. **B400**, 169 (1997), hep-lat/9701008.
- [49] Y. Iwasaki, K. Kanaya, S. Kaya, S. Sakai, and T. Yoshie, Phys. Rev. **D69**, 014507 (2004), hep-lat/0309159.
- [50] S. Catterall and F. Sannino, Phys. Rev. **D76**, 034504 (2007), 0705.1664.
- [51] T. Appelquist, G. T. Fleming, and E. T. Neil, Phys. Rev. Lett. **100**, 171607 (2008), 0712.0609.
- [52] A. Deuzeman, M. P. Lombardo, and E. Pallante, Phys. Lett. **B670**, 41 (2008), 0804.2905.
- [53] A. Deuzeman, M. P. Lombardo, and E. Pallante (2009), 0904.4662.
- [54] T. Appelquist, G. T. Fleming, and E. T. Neil, Phys. Rev. **D79**, 076010 (2009), 0901.3766.
- [55] Z. Fodor, K. Holland, J. Kuti, D. Negradi, and C. Schroeder, Phys. Lett. **B681**, 353 (2009), 0907.4562.
- [56] Z. Fodor, K. Holland, J. Kuti, D. Negradi, and C. Schroeder (2009), 0911.2463.
- [57] E. Pallante (2009), 0912.5188.
- [58] T. DeGrand (2010), 1010.4741.
- [59] V. A. Miransky and K. Yamawaki, Mod. Phys. Lett. **A4**, 129 (1989).
- [60] R. S. Chivukula, Phys. Rev. **D55**, 5238 (1997), hep-ph/9612267.
- [61] T. Appelquist and F. Sannino, Phys. Rev. **D59**, 067702 (1999), hep-ph/9806409.
- [62] V. L. Berezinskii, Sov. Phys. JETP **32**, 493 (1971).
- [63] V. L. Berezinskii, Sov. Phys. JETP **34**, 610 (1972).
- [64] J. M. Kosterlitz and D. J. Thouless, J. Phys. **C6**, 1181 (1973).
- [65] D. B. Kaplan, J.-W. Lee, D. T. Son, and M. A. Stephanov, Phys. Rev. **D80**, 125005 (2009), 0905.4752.
- [66] J. Braun and H. Gies, JHEP **05**, 060 (2010), 0912.4168.
- [67] M. Jarvinen and F. Sannino (2010), 1009.5380.
- [68] T. DeGrand and A. Hasenfratz, Phys. Rev. **D80**, 034506 (2009), 0906.1976.
- [69] L. Del Debbio and R. Zwicky, Phys. Rev. **D82**, 014502 (2010), 1005.2371.
- [70] L. Del Debbio and R. Zwicky (2010), 1009.2894.
- [71] J. Braun (2006), hep-ph/0611145.
- [72] H. Gies, J. Jaeckel, and C. Wetterich, Phys. Rev. **D69**, 105008 (2004), hep-ph/0312034.
- [73] H. S. Fukano and F. Sannino, Phys. Rev. **D82**, 035021 (2010), 1005.3340.
- [74] J. Braun, H. Gies, and D. D. Scherer (2010), 1011.1456.
- [75] J. Braun, Phys. Rev. **D81**, 016008 (2010), 0908.1543.
- [76] R. D. Pisarski and F. Wilczek, Phys. Rev. **D29**, 338 (1984).
- [77] C. Wetterich, Phys. Lett. **B301**, 90 (1993).

- [78] M. Reuter (1996), hep-th/9602012.
- [79] D. F. Litim and J. M. Pawłowski (1998), hep-th/9901063.
- [80] C. Bagnuls and C. Bervillier, Phys. Rept. **348**, 91 (2001), hep-th/0002034.
- [81] J. Berges, N. Tetradis, and C. Wetterich, Phys. Rept. **363**, 223 (2002), hep-ph/0005122.
- [82] J. Polonyi, Central Eur. J. Phys. **1**, 1 (2003), hep-th/0110026.
- [83] B. Delamotte, D. Mouhanna, and M. Tissier, Phys. Rev. **B69**, 134413 (2004), cond-mat/0309101.
- [84] J. M. Pawłowski, Annals Phys. **322**, 2831 (2007), hep-th/0512261.
- [85] H. Gies (2006), hep-ph/0611146.
- [86] B. Delamotte (2007), cond-mat/0702365.
- [87] O. J. Rosten (2010), 1003.1366.
- [88] D. U. Jungnickel and C. Wetterich, Phys. Rev. **D53**, 5142 (1996), hep-ph/9505267.
- [89] D. F. Litim, Phys. Lett. **B486**, 92 (2000), hep-th/0005245.
- [90] D. F. Litim, Phys. Rev. **D64**, 105007 (2001), hep-th/0103195.
- [91] D. F. Litim, Int. J. Mod. Phys. **A16**, 2081 (2001), hep-th/0104221.
- [92] M. Reuter and C. Wetterich, Nucl. Phys. **B417**, 181 (1994).
- [93] H. Gies, Phys. Rev. **D66**, 025006 (2002), hep-th/0202207.
- [94] J. M. Pawłowski, D. F. Litim, S. Nedelko, and L. von Smekal, Phys. Rev. Lett. **93**, 152002 (2004), hep-th/0312324.
- [95] T. van Ritbergen, J. A. M. Vermaseren, and S. A. Larin, Phys. Lett. **B400**, 379 (1997), hep-ph/9701390.
- [96] M. Czakon, Nucl. Phys. **B710**, 485 (2005), hep-ph/0411261.
- [97] U. Ellwanger, Phys. Lett. **B335**, 364 (1994), hep-th/9402077.
- [98] L. von Smekal, R. Alkofer, and A. Hauck, Phys. Rev. Lett. **79**, 3591 (1997), hep-ph/9705242.
- [99] L. von Smekal, A. Hauck, and R. Alkofer, Ann. Phys. **267**, 1 (1998), hep-ph/9707327.
- [100] C. Lerche and L. von Smekal, Phys. Rev. **D65**, 125006 (2002), hep-ph/0202194.
- [101] R. Alkofer, C. S. Fischer, and F. J. Llanes-Estrada, Phys. Lett. **B611**, 279 (2005), hep-th/0412330.
- [102] C. S. Fischer, A. Maas, and J. M. Pawłowski, Annals Phys. **324**, 2408 (2009), 0810.1987.
- [103] C. S. Fischer and J. M. Pawłowski, Phys. Rev. **D80**, 025023 (2009), 0903.2193.
- [104] C. S. Fischer and J. M. Pawłowski, Phys. Rev. **D75**, 025012 (2007), hep-th/0609009.
- [105] A. C. Aguilar, D. Binosi, J. Papavassiliou, and J. Rodriguez-Quintero, Phys. Rev. **D80**, 085018 (2009), 0906.2633.